Endosome dynamics regulated by a Rho protein

Carol Murphy*, Rainer Saffrich, Maika Grummt*, Hélène Gournier, Vladimir Rybin, Mariantonietta Rubino, Petri Auvinen*, Anne Lütcke, Robert G. Parton* & Marino Zerial

European Molecular Biology Laboratory, Postfach 10.2209, Meyerhofstrasse 1, 69012 Heidelberg, Germany

Vesicular transport is a dynamic process that requires coordinated interactions between membrane and cytoskeleton. The mechanisms and molecules integrating these interactions are unclear. A Rho protein, RhoD, might provide a molecular link between membrane traffic and the cytoskeleton. Activated RhoD causes rearrangements of the actin cytoskeleton and cell surface, and governs early endosome motility and distribution.

MEMBRANE transport is necessary for the biogenesis and maintenance of organelles and the transport of proteins and lipids through the secretory and endocytic pathways. Vesicular transport between organelles occurs in an environment whose shape, flexibility and organization is controlled by the cytoskeleton. Microtubules and actin filaments have been increasingly linked to the general eukaryotic transport apparatus. Actin is implicated in the development and maintenance of polarized growth in yeast[1], and in endocytosis in yeast[2] and mammalian polarized epithelial cells[3,4]. Microtubules are involved in vesicular transport[5], and are thought to control long-range bi-directional movement[6].

Small GTPases are involved in many cellular processes[7]. Rab proteins regulate vesicular docking and fusion at various steps of biosynthetic and endocytic transport[8–11], and GTPases of the Rho family regulate the actin cytoskeleton. Rho proteins transduce signals from plasma membrane receptors and control cell adhesion, motility and shape, as well as bud assembly and polarized growth in yeast and *Drosophila*[12–17]. Rho proteins are also thought to participate in membrane transport. RhoA regulates clathrin-independent endocytosis in *Xenopus* oocytes[18], and activated mutants of RhoA and Rac1 impede the formation of clathrin-coated vesicles at the plasma membrane in mammalian cells[19]. However, the role of Rho proteins in organelle dynamics has not been explored.

Here we present the protein RhoD, which regulates early endosome dynamics and distribution, and causes rearrangements of the cell surface and actin cytoskeleton. We propose that RhoD is a good candidate for a molecule that coordinates membrane transport with the function of the cytoskeleton.

Background

A cloning approach based on the polymerase chain reaction (PCR) indicated the existence of a new member of the Rho protein family[20]. To investigate its function we obtained a complementary DNA clone encoding the full-length protein and determined the nucleotide and deduced amino-acid sequence (Fig. 1*a*). Comparison of this sequence to the known members of the Rho family indicates a homology of 56–67%. We called this protein RhoD, because this analysis indicates that it is not an isoform but rather a distinct member of the Rho family, more closely related to the RhoA, B, C group than to Rac and Cdc42. The protein is widely expressed in mouse tissues (Fig. 1*b*).

Changes to the actin cytoskeleton

To investigate the function of RhoD, we transiently expressed in BHK cells the wild-type protein RhoD, $RhoD^{G26V}$ (a mutant deficient in GTP hydrolysis) and $RhoD^{T31N}$ (a mutant stabilized in the GDP-bound form), using the T7 vaccinia virus system[21]. Striking alterations of cell morphology were observed in cells expressing both RhoD and $RhoD^{G26V}$ (Fig. 2*a–c*). These cells show thin processes reaching lengths of 20–30 μm, some of which are firmly attached to the substratum, whereas others are motile. By time-lapse video microscopy we captured the growth of the extensions (see Supplementary Information), which are commonly observed (70%) among the transfected cells. F-actin was abundant in the structures (Fig. 2*d*), but microtubules were absent (data not shown). This effect is not restricted to BHK cells, as HeLa, NIH3T3, NRK and J774 cells exhibited the same phenotype. It is also not a result of the expression system used, as: (1) hydroxyurea was used to inhibit virus assembly, avoiding changes in the actin cytoskeleton[21,22]; (2) non-viral-mediated transient expression of RhoD gave similar results (data not shown); (3) expression of $RhoD^{T31N}$ induced minimal changes in cell morphology; and (4) activated mutants of Cdc42 and Rac1 similarly expressed did not exhibit the same effects as RhoD, but did cause the same phenotypic alterations on the actin cytoskeleton as reported[15,16] (data not shown).

The plasma membrane rearrangements induced by RhoD and $RhoD^{G26V}$ were accompanied by alterations of the actin cytoskeleton. In cells expressing wild-type or mutant RhoD (Fig. 2*c*), the actin stress fibres disappear from the cell body (Fig. 2*d*), although they remain intact in untransfected control cells (Fig. 2*e*), in cells expressing an unrelated protein (Fig. 2*f*, *g*) or in $RhoD^{T31N}$ (data not shown) under the same conditions. However, stress fibres were not stimulated by Rho^{V14} using our expression system (not shown). As in the case of stress fibres, we found that focal adhesion-associated proteins, paxillin (Fig. 3), vinculin and phosphotyrosine-containing proteins (data not shown), disassemble from the cell periphery on expression of RhoD or $RhoD^{G26V}$ proteins. In contrast, the focal adhesions are still intact in cells expressing $RhoD^{T31N}$ (data not shown), $Rac1^{V12}$ and $Cdc42^{V12}$ (Fig. 3), as previously described[16]. We did not observe the presence of the above adhesion markers in the plasma-membrane processes formed by RhoD (Fig. 3*a*).

* Present addresses: Laboratory of Biological Chemistry, University of Ioannina Medical School, 45110 Ioannina, Greece (C.M.); Institute for Cell Biology, Schiller strasse 42, 80336 Munich, Germany (M.G.); Institute of Biotechnology, University of Helsinki, P.O. Box 56, 00014 Helsinki, Finland (P.A.); and Centre for Microscopy and Microanalysis, Department of Physiology and Pharmacology, and Centre for Molecular and Cellular Biology, University of Queensland, Queensland 4072, Brisbane, Australia (R.G.P.).

Regulation of early endosome dynamics

We next investigated the localization of RhoD in BHK cells overexpressing the myc-tagged protein. By a combination of confocal immunofluorescence and electron microscopy, RhoD was localized to the plasma membrane (Fig. 2*h*; this staining is not apparent following the extraction procedure for immunofluorescence) and vesicular structures throughout the cell (Fig. 4). Immunogold labelling also revealed an enrichment on putative endosomal compartments (data not shown). This localization was examined by confocal microscopy in BHK cells coexpressing the RhoD^{G26V} protein with the human transferrin receptor. Fluorescein isothiocyanate (FITC)-labelled transferrin, internalized for 15 min, almost completely colocalized with RhoD, verifying that the labelled structures are indeed on the early endocytic/recycling pathway (Fig. 4) and perinuclear recycling compartment[23,24] (Fig. 4*b*, hash symbol). Moreover, overexpressed RhoD^{G26V} altered the intracellular distribution and organization of early endosomes. First, early endosomes were more dispersed throughout the cell and extended into the RhoD-induced, actin-containing processes (Fig. 4*c–f*). Second, a striking alignment of early endosomes was often observed on expression of RhoD^{G26V} (Fig. 4*b*). Third, the endosomes appeared less pleiomorphic and to a lesser extent connected by tubular processes than control cells. Electron-microscopy analysis indicated that the endosomes appear spherical, lacking the tubular extensions evident on control endosomes (Fig. 5).

To investigate whether RhoD could kinetically modify endocytic transport, we tested the effect of RhoD and RhoD^{G26V} on the transferrin cycle *in vivo*. The number of surface transferrin receptors and the kinetics of internalization were unaltered. Transferrin recycling was decreased by approximately 10% (data not shown). Thus RhoD does not significantly affect the kinetics of transport from the plasma membrane to the early endosomes and along the recycling pathway. These data suggest that RhoD plays a different role in the dynamics of this compartment, such as regulating homotypic fusion, fission and/or motility. To allow the visualization of this process, we used the property of Rab5 which regulates early endosome homotypic fusion *in vitro*[25] and *in vivo*[21]. Expression of the GTPase-deficient mutant Rab5^{Q79L} stimulates early endosome homotypic fusion and induces the appearance of enlarged endosomes[26] (Fig. 6*a*, 7*a*). To investigate the role of RhoD in endosome function we coexpressed Rab5a^{Q79L} with RhoD, RhoD^{G26V} or RhoD^{T31N}. When Rab5a^{Q79L} is expressed alone, large early endosomes are formed and accumulate around the nucleus[26], and actin is recruited around the enlarged endosomes (Fig. 7*b*). When Rab5a^{Q79L} and wild-type RhoD (Fig. 6*a–c*) or RhoD^{T31N} (data not shown) are coexpressed, the enlarged early endosomes are not altered in size or location. Actin is recruited around the Rab5-positive, large early endosomes (Fig. 6*c*), and RhoD is also localized to the endosomal membrane (Fig. 6*b*). In contrast, coexpression of RhoD^{G26V} and Rab5a^{Q79L} abolishes the expansion of the endosomes, which are no longer perinuclear but appear scattered throughout the cell (Fig. 6*d–f*). Surprisingly, in view of the effect of RhoD and RhoD^{G26V} on the disassembly of actin stress fibres, actin is still localized around the structures formed. Therefore the RhoD mutant protein neither prevents the recruitment of actin around, nor induces the disassembly of actin from, the endosomal membrane.

We performed two control experiments to exclude the possibility of a nonspecific effect of RhoD on the actin cytoskeleton. First, treatment of cells with 1 μg ml^{-1} cytochalasin D, which causes F-actin depolymerization (Fig. 7*d*), had no effect on the formation of the endosomal structures or on their maintenance (Fig. 7*c*). Second, activated mutants of other members of the Rho protein family with established effects on the actin cytoskeleton, Rac1^{V12} (Fig. 6*g*), Cdc42^{V12} (Fig. 6*h*) or RhoA^{V14} (Fig. 6*i*), did not impede the effects of Rab5a^{Q79L} on endosomal morphology. Thus

a

```
1   MNASQVAGEEAPQSGHSVKVVLVGDGGCGKTSLMMVFAK
40  GAFPESYSPTVFERYNATLQMKGKPVHLQIWDTAGQDDYD
80  RLRPLFYPDANVLLLCFDVTNPNSFDNVSNRWYPEVTHFCK
121 GVPIIVVGCKIDLRKDKVLVNNLRKKRLEPVTYHRGHDMA
161 RSVGAVAYLECSARLHDNVEAVFQEAAEVALSSRRHNFWR
201 RITQNCCLAT*
```

b

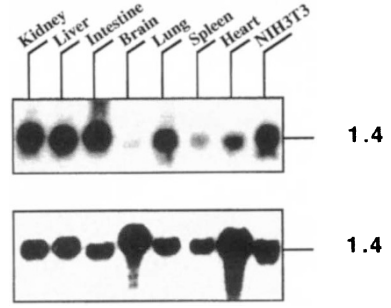

FIG. 1 Sequence and expression pattern of RhoD. *a*, Amino-acid sequence of mouse RhoD. Consensus motifs GXXXXGK[S,T] and DTAGQ are underlined. NKXDL, a conserved motif involved in GTP binding, is replaced in RhoD by CKIDL, underlined. The CAAX motif undergoing prenylation in RhoD is CCLAT, underlined. The asparagine residue in Rho proteins, the modification site for botulinum ADP-ribosyltransferase[12,33], is replaced in RhoD by arginine, white letter. *b*, Northern blot analysis of total RNA from adult mouse organs hybridized with RhoD cDNA and glyceraldehyde 3-phosphate dehydrogenase (GAPDH) to control loading and RNA quality. RNA markers are indicated.

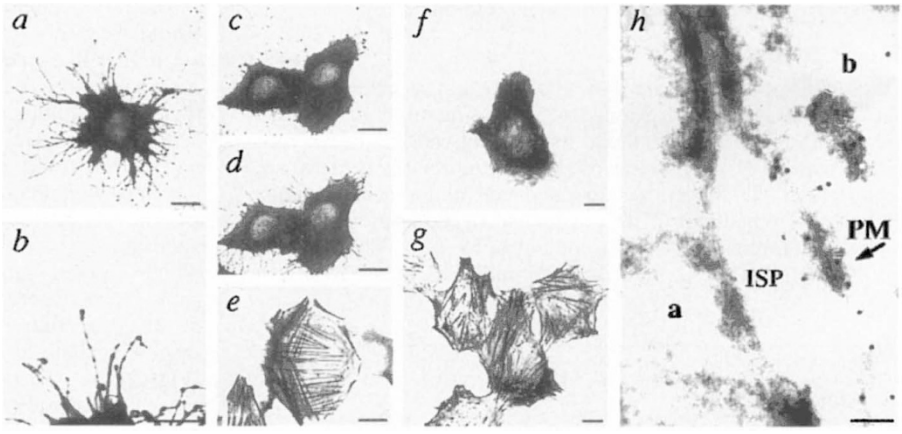

FIG. 2 RhoD induces plasma-membrane process formation, alters actin stress fibres, and localizes to the plasma membrane. *a*, BHK cell expressing myc-tagged RhoD^{G26V} visualized by indirect immunofluorescence. *b*, Higher magnification of membrane processes. *c*, NRK cells expressing RhoD^{G26V} labelled with an antibody recognizing myc-tagged RhoD^{G26V} and *d*, rhodamine-labelled phalloidin. *e*, Stress fibres in a control cell. *f*, NRK cells expressing myc-Rab17 stained with rhodamine-labelled phalloidin. *g*, Immunoelectron microscopy on BHK cells expressing myc-tagged RhoD. *h*, Overview of a transfected (b) and a control cell (a). ISP, intercellular space; PM, plasma membrane. Scale bars: *a–g*, 10 μm; *h*, 100 nm.

the effect on early endosomes seen with RhoD^{G26V} is highly specific.

RhoD regulates endosome motility

To investigate the mechanism by which RhoD interferes with the formation of the large endosomes in response to Rab5^{Q79L}, we monitored this process by time-lapse video microscopy. In cells expressing the Rab5^{Q79L} mutant alone we observed rapid vesicle motility (see Supplementary Information). Endosome movement facilitated the contact between endocytic vesicles, causing progressive enlargement of endosomes by homotypic fusion at the cell periphery and movement towards the nucleus (see, for example, the movement and fusion of endosomes indicated by arrowheads in Fig. 8, panels 1–6). This analysis further indicated that endosomes become less motile as they grow. Homotypic fusion between endosomes seems to be asymmetrical, with one endosome expanding by assimilating the other (Fig. 8, panels 5, 6). In contrast, endosome motility was severely reduced in cells coexpressing Rab51^{Q79L} and RhoD^{G26V} (Fig. 8, panels 7, 8) (see Supplementary Information). Consistent with the immunofluorescence analysis (Fig. 4), the motionless endosomes were spread throughout the cells with extended processes. Occasionally, when contact occurred, endosomal fusion events were observed (see Supplementary Information), but it seems that the reduced endosomal motility caused by RhoD^{G26V} might prevent the excessive fusion activity enhanced by Rab5a^{Q79L} alone. Cytosol containing overexpressed RhoD or RhoD^{G26V} did not inhibit the homotypic fusion between early endosomes *in vitro* (data not shown), lending further support to the idea that RhoD does not act at the fusion stage. These results therefore suggest that the alterations of RhoD^{G26V} on the endosome dynamics are primarily due to an inhibition of intracellular motility of this organelle.

Discussion

Rho proteins share the property of regulating the actin cytoskeleton but they have different effects on actin organization. Expression of RhoA promotes assembly of stress fibres[14], Rac1 generates lamellipodia[15], and Cdc42 triggers actin polymerization and induces filopodia[16]. We have identified RhoD, a protein that is localized to the plasma membrane and early endosomes. When overexpressed, RhoD and RhoD^{G26V} induce F-actin-containing membrane processes and the disassembly of stress fibres and focal adhesions from the cell periphery. The effects of RhoD are, therefore, in sharp contrast to those induced by the other Rho family members. Furthermore, RhoD plays an important role in endosome organization. RhoD^{G26V} causes scattering of the endosmes throughout the cell and impairs Rab5a^{Q79L}-stimulated homotypic fusion.

We sought to identify the mechanism by which RhoD affects early endosome dynamics. Unlike Rho and Rac[19], RhoD did not alter the kinetics of receptor-mediated endocytosis and recycling. Moreover, neither wild-type RhoD or RhoD^{G26V} interferes with the homotypic fusion between early endosomes in a standard *in vitro* assay (data not shown), which depends on Rab5 activity[25] excluding a direct inhibitory effect on the fusion step. Time-lapse video microscopy analysis suggested a different explanation: the RhoD mutant seems to exert its effect by inhibiting organelle motility. This does not necessarily imply that RhoD is an inhibitor of endosome dynamics, but rather that its normal GTP/GDP cycling (perturbed in the mutant) regulates this activity. In a dynamic equilibrium between fusion and fission, the RhoD

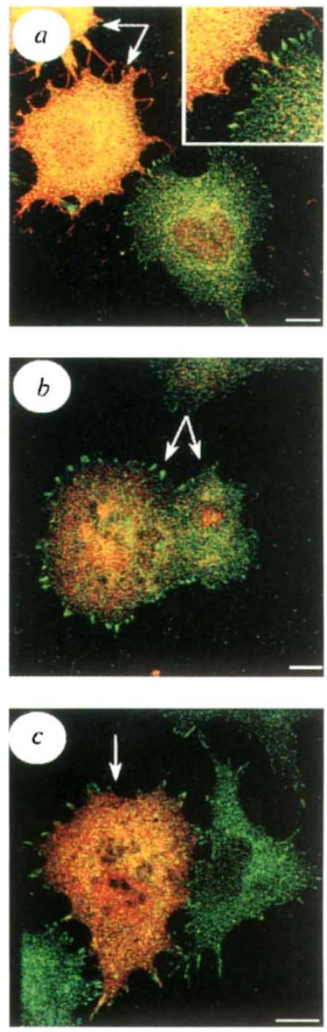

FIG. 3 Paxillin localization in BHK cells expressing RhoD^{G26V}. BHK cells were either transfected with RhoD^{G26V} (*a*), Rac1^{V12} (*b*), or Cdc42^{V12} (*c*). Double immunofluorescence was performed to detect RhoD (*a*), Rac1 (*b*) or Cdc42 (*c*) and paxillin. Only the overlays are shown here; RhoD, Rac1 and Cdc42 are visualized in red–orange colour, and paxillin in green. Arrows indicate the transfected cells. The insert in *a* is a higher magnification to demonstrate the loss of paxillin localization at the cell periphery in the cell expressing RhoD^{G26V}. Scale bars, 10 μm.

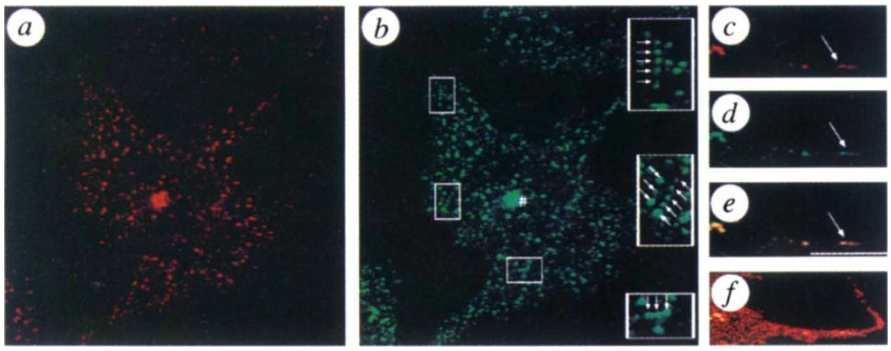

FIG. 4 Localization of RhoD and internalized FITC-labelled transferrin, which was internalized for 15 min at 37 °C in BHK cells expressing RhoD^{G26V} and the human transferrin receptor. *a*, RhoD^{G26V} staining, and *b*, FITC-labelled transferrin. In *b*, arrows indicate aligned endosomes with inserts showing magnifications of these areas; the hash sign indicates the perinuclear recycling endosome. *c*–*f*, Membrane processes formed upon expression of RhoD^{G26V}. *c*, RhoD^{G26V} staining; *d*, FITC-labelled transferrin; and *e*, the overlay of *c* and *d*. *f*, This image has a pseudocolour to demonstrate the shape of the membrane process. Scale bar, 10 μm.

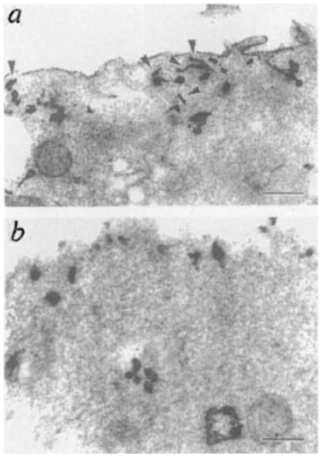

FIG. 5 Morphological alteration of early endosomes in cells expressing RhoD^{G26V}. *a*, Control BHK cells showing early endosomes with several tubular connections (arrowheads). *b*, In BHK cells expressing RhoD^{V26G}, endosomes are spherical and lack tubular connections. Scale bars, 250 nm.

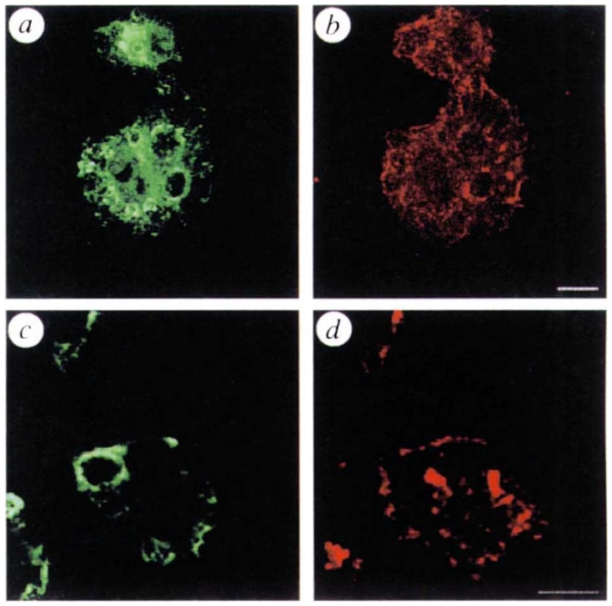

FIG. 7 Effect of cytochalasin D on the formation and maintenance of the enlarged endosomes formed by Rab5a^{Q79L}. BHK cells were transfected with a plasmid encoding Rab5a^{Q79L}. 30 min after transfection, 1 μg ml^{-1} cytochalasin D was added to half of the samples, and the others were allowed to express the protein in the absence of the drug as a control. The cells were fixed and processed for immunofluorescence 4 h after transfection. In control cells, *a*, Rab5 staining, and *b*, the F-actin. In cells treated with cytochalasin D, *c*, Rab5 staining, and *d*, the F-actin. Scale bars, 10 μm.

mutant might shift the balance towards fission, dispersing the endosomes and decreasing the tubular connections (Figs 4 and 5). Endosome motility might be important, for example in the case of cell migration, where membrane dynamics are critical and adhesion molecules and surface receptors are internalized at the rear of the cell and recycled to the leading edge (see refs 27–29 for reviews).

It is likely that RhoD function depends on the cytoskeleton,

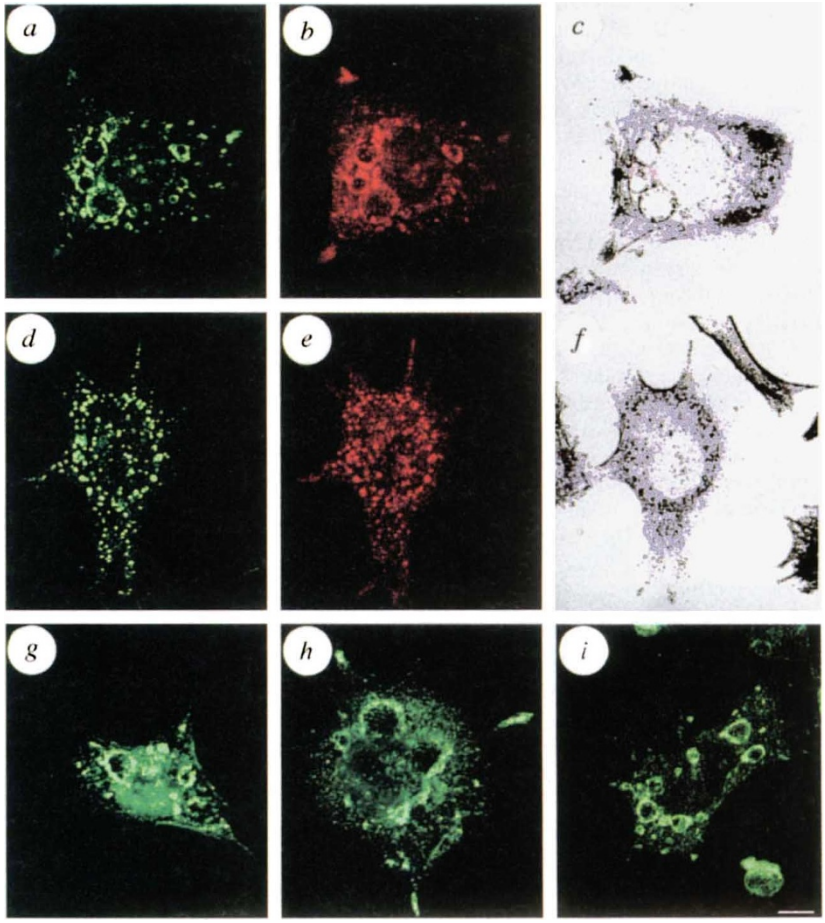

FIG. 6 Effect of RhoD and RhoD^{G26V} on early endosome enlargement induced by Rab5a^{Q79L}. BHK cells were co-transfected with Rab5a^{Q79L} and either RhoD (*a*–*c*) or RhoD^{G26V} (*d*–*f*). Immunofluorescence staining of Rab5a (*a*, *d*), RhoD (*b*, e), and rhodamine phalloidin to visualize F-actin (*c*–*f*). BHK cells were co-transfected with Rab5a^{Q79L} and Rac1^{V12} (*g*), Cdc42^{V12} (*h*) or RhoA^{V14} (*i*). Only the Rab5a staining is shown. Scale bar, 10 μm.

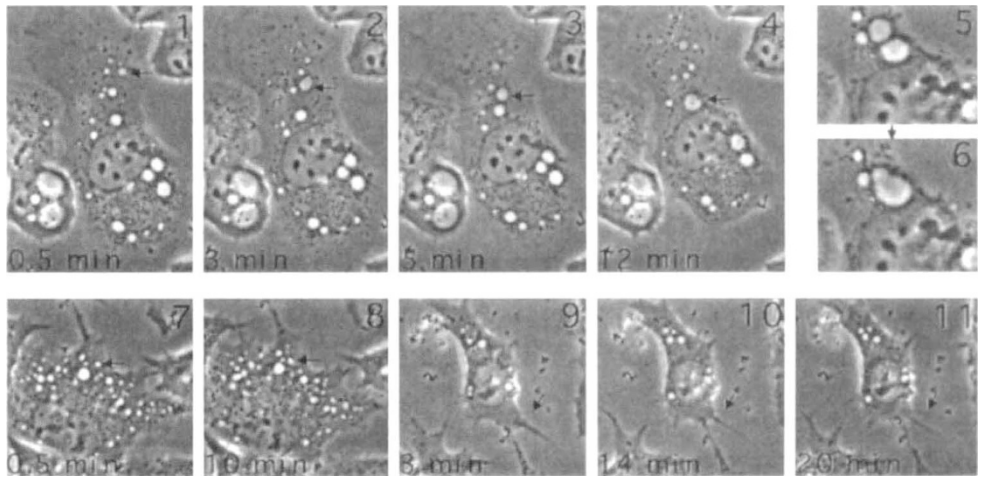

FIG. 8 Time-lapse video microscopy of BHK cells expressing Rab5a^{Q79L} (panels 1–6) or coexpressing Rab5a^{Q79L} and RhoD^{G26V} (panels 7–11) (see Supplementary Information). Panels 5 and 6 show asymmetric endosome fusion. Panels 9–11 show membrane process extension in a cell coexpressing Rab5a^{Q79L} and RhoD^{G26V}. Panels 1–4 are 62 μm × 89 μm; panels 7–11 are 63 μm × 63 μm.

given its effect on actin organization, and the observation that the endosomes are often aligned suggests movement along cytoskeletal filaments. Despite the lack of effect of cytochalasin D on endosome expansion (Fig. 7), actin remains one obvious candidate. Indeed, although this drug disrupts the supramolecular organization of the actin network, it is not clear whether all filaments are affected equally[30]. In this respect, it is noteworthy that, under conditions where actin stress fibres disassemble upon RhoD expression, actin remains associated with the endosomal membrane. The discovery of unconventional myosins containing GAP domains for Rho proteins[31,32] also suggests that actin may be involved. However, the movement of the endosomes towards the perinuclear region suggests that microtubules also participate, and it is conceivable that both types of filaments could be sequentially involved. Our findings showing that RhoD exerts a regulatory role on the actin cytoskeleton and endosome dynamics provide direction for further studies intended to unravel the mechanisms governing the interactions between membrane and cytoskeleton. □

Methods

Cloning of rhoD, generation of expression constructs, and northern blot analysis. In a PCR screen to identify new GTP-binding proteins a PCR fragment encoding a Rho-related protein was isolated[20]. Using a combination of 5′ and 3′ rapid amplification of cDNA ends (RACE)[34], the entire coding region was isolated from mouse kidney RNA. After cDNA synthesis using oligo dT, the 5′ end was tailed with poly(G) residues and PCR was performed using primer 5′-CAGGTTTACCCTTCATCTG-3′ specific for RhoD, and an upstream poly(C) primer. A second round of PCR used a nested antisense RhoD-specific primer, 5′-TCGAGGATCCAGAGTGGCATTATAGCGC-3′ and the upstream poly(C) primer. To extend the 3′ end, a first round of PCR was carried out using an upstream sense primer in RhoD 5′-CCTTCCCAGAGAGCTACAG-3′ and a 3′ oligo dT primer. A second round of PCR used a nested sense primer in the RhoD sequence 5′-GCCGAATTCGGATCCAGAGCTACAGTCCCACAGTGTTTGA-3′. RhoD cDNA was cloned in frame into the pGEM 1 vector containing the c-*myc* tag (pGEM-myc) at the 5′ end. The G26V mutant of RhoD was constructed by PCR using the oligonucleotide 5′-GGTGGGCGACGTGGGCTGCGGG-3′, according to ref. 35 and cloned into pGEM-myc. Rac1^{V12} and RhoA^{V14} were subcloned into pGEM-myc. Cdc42^{V12} was constructed and cloned into pGEM-myc for expression. For northern blot analysis, total RNA was isolated from adult mouse organs according to standard procedures. Total RNA (25 μg) was loaded on a formaldehyde gel, transferred to Genescreen plus membrane and probed with a PCR fragment corresponding to the 3′ end of the cDNA.

Immunofluorescence. BHK cells were transiently transfected, fixed and immunofluorescence performed essentially as described[21]. To detect the myc-tagged proteins, the 9E10 monoclonal antibody (ATCC19) was used. To visualize the actin stress fibres, rhodamine-labelled phalloidin (Molecular Probes) was added with the secondary antibodies (Dianova). Staining with Rab5a polyclonal antibody was as described[36]. Polyclonal rabbit antiserum was raised against histidine-tagged RhoD expressed in *Escherichia coli*. In the experiment of Fig. 3, rabbit polyclonal antibodies against RhoD, Rac1 (Santa Cruz, used at 1:50 dilution) or Cdc42 (as described in ref. 35 and used at 1:50 dilution) and a monoclonal antibody recognizing paxillin (Zymed, used at 1:50 dilution) were used. Cy5-labelled anti-mouse secondary antibody was a gift from S. Reinsch and was used at 1:50 dilution. Samples were visualized using the EMBL confocal scanning laser-beam microscope[37]. The 529, 476 and 633 laser lines of the Argon-ion laser were used for excitation of rhodamine, fluorescein and cy5-labelled samples, respectively. Images were recorded and imported into either Adobe Photoshop or NIH Image graphic programs for compilation.

Electron microscopy. For immunoelectron microscopy, BHK cells were transfected as described[21], fixed in 8% paraformaldehyde in 250 mM HEPES, pH 7.35, scraped from the culture dish, pelleted and processed for cryosectioning[38]. Thawed sections were labelled by sequential incubations with the 9E10 culture supernatant, followed by secondary antibody and 10-nm protein A-gold. To compare the morphology of the endosomes after expression of RhoD^{G26V}, we co-transfected this DNA and human transferrin receptor. After 4 h, cells were washed and incubated continuously for 5 min with 25 μg ml^{-1} human transferrin conjugated to peroxidase. At this concentration only those cells expressing a high level of transferrin receptor are labelled.

FITC transferrin uptake. BHK cells were infected as described[21], and co-transfected with plasmids encoding RhoD^{G26V} and the human transferrin receptor. 4 h after transfection (the medium was devoid of serum), the coverslips were incubated in a humidified chamber with 50 μg ml^{-1} FITC-labelled transferrin for 15 min at 37 °C. Coverslips were then rinsed in PBS and fixed in 3% PFA, permeabilized in 0.1% triton, and the 9E10 monoclonal antibody recognizing the myc-tagged RhoD was added, followed by rhodamine-labelled donkey anti-mouse IgG.

Time-lapse video microscopy. BHK cells were transfected as above, and 2 h later cyclohexamide was added for 1 h (ref. 21). Cells were washed 8 times for 1 min to remove the cyclohexamide, and video microscopy was carried out using a Zeiss Axiovert 10 inverted microscope equipped with a cooled slow-scan CCD (charge-coupled device) camera (Photometrics CH250) connected to a SUN workstation. Images were acquired every 30 s at 37 °C with low light exposure, at ×63 magnification (Zeiss Plan-Apochromat lens, 63 × 1.4). A series of 30–100 images were taken, corresponding to 15–50 min of observation. The images were processed and animated using the software package KHOROS and NIH-Image.

Received 23 August; accepted 9 October 1996.

1. Novick, P. & Botstein, D. *Cell* **40,** 405–416 (1985).
2. Riezman, H. *Trends Cell Biol.* **3,** 273–277 (1993).
3. Gottlieb, T. A., Ivanov, I. E., Adesnik, M. & Sabatini, D. D. *J. Cell Biol.* **120,** 695–710 (1993).
4. Jackman, M. R., Shurety, W., Ellis, J. A. & Luzio, J. P. *J. Cell Sci.* **107,** 2547–2556 (1994).
5. Cole, N. B. & Lippincott-Schwartz, J. *Curr. Opin. Cell Biol.* **7,** 55–64 (1995).
6. Allan, V. *FEBS Lett.* **369,** 101–106 (1995).
7. Bourne, H. R., Sanders, D. A. & McCormick, F. *Nature* **348,** 125–132 (1990).
8. Zerial, M. & Stenmark, H. *Curr. Opin. Cell Biol.* **5,** 613–620 (1993).
9. Ferro-Novick, S. & Novick, P. *Annu. Rev. Cell Biol.* **9,** 575–599 (1993).
10. Nuoffer, C. & Balch, W. E. *Annu. Rev. Biochem.* **63,** 949–990 (1994).
11. Pfeffer, S. R. *Curr. Opin. Cell Biol.* **6,** 522–526 (1994).
12. Chardin, P. *et al. EMBO J.* **8,** 1087–1092 (1989).
13. Adams, A. E. M., Johnson, D. I., Longnecker, R. M., Sloat, B. F. & Pringle, J. R. *J. Cell Biol.* **111,** 131–142 (1990).
14. Ridley, A. J. & Hall, A. *Cell* **70,** 389–399 (1992).
15. Ridley, A. J., Paterson, H. F., Johnston, C. L., Diekmann, D. & Hall, A. *Cell* **70,** 401–410 (1992).
16. Nobes, C. D. & Hall, A. *Cell* **81,** 53–62 (1995).
17. Eaton, S., Auvinen, P., Luo, L., Jan, Y. N. & Simons, K. *J. Cell Biol.* **131,** 151–164 (1995).
18. Schmalzing, G. *et al. J. Cell Biol.* **130,** 1319–1332 (1995).
19. Lamaze, C., Chuang, T.-H., Terlecky, L. J., Bokoch, G. M. & Schmid, S. L. *Nature* **382,** 177–179 (1996).
20. Chavrier, P., Simons, K. & Zerial, M. *Gene* **112,** 261–264 (1992).
21. Bucci, C. *et al. Cell* **70,** 715–728 (1992).

22. Cudmore, S., Cossart, P., Griffiths, G. & Way, M. *Nature* **378,** 636–638 (1995).
23. Yamashiro, D. J. & Maxfield, F. R. *Cell* **37,** 389–400 (1984).
24. Hopkins, C. R., Gibson, A., Shipman, M., Strickland, D. K. a. & Trowbridge, I. S. *J. Cell Biol.* **125,** 1265–1274 (1994).
25. Gorvel, J.-P., Chavrier, P., Zerial, M. & Gruenberg, J. *Cell* **64,** 915–925 (1991).
26. Stenmark, H. *et al. EMBO J.* **13,** 1287–1296 (1994).
27. Sheetz, M. P. & Dai, J. *Trends Cell Biol.* **6,** 85–89 (1996).
28. Lauffenburger, D. A. & Horwitz, A. F. *Cell* **84,** 359–369 (1996).
29. Mitchinson, T. J. & Cramer, L. P. *Cell* **84,** 371–379 (1996).
30. Cooper, J. A. *J. Cell Biol.* **105,** 1473–1478 (1987).
31. Reinhard, J. *et al. EMBO J.* **14,** 697–704 (1995).
32. Wirth, J. A., Jensen, K. A., Post, P. L., Bement, W. M. & Mooseker, M. S. *J. Cell Sci.* **109,** 653–661 (1996).
33. Sekine, A., Fujiwara, M. & Narumiya, S. *J. Biol. Chem.* **264,** 8602–8605 (1989).
34. Frohman, M. A., Dush, M. K. & Martin, G. R. *Proc. Natl Acad. Sci. USA* **85,** 8998–9002 (1988).
35. Landt, O., Grunert, H.-P. & Hahn, U. *Gene* **96,** 125–128 (1990).
36. Chavrier, P., Parton, R. G., Hauri, H. P., Simons, K. & Zerial, M. *Cell* **62,** 317–329 (1990).
37. Stelzer, E. H. K., Stricker, R., Pick, R., Storz, C. & Hanninen, P. *Proc. Soc. Photo-opt. Instrum. Eng.* **1028,** 146–151 (1989).
38. Griffiths, G., McDowall, A., Back, R. & Dubochet, J. *J. Ultrastruct. Res.* **89,** 65–78 (1984).

SUPPLEMENTARY INFORMATION is available on *Nature*'s World-Wide Web site (http://www.nature.com) or as videos from Mary Sheehan at the London editorial office of *Nature*.

ACKNOWLEDGEMENTS. We thank A. Habermann and G. Griffiths for the electron-microscopy analysis of RhoD^{G26V}-expressing cells; S. Reinsch, E. Stelzer and N. Salmon for advice on confocal microscopy and data processing; A. Giner and M. Stapleton for technical assistance; A. Hall for the Rac1^{V12} plasmid; and J. Burkhardt, M. Glotzer, S. Reinsch, K. Simons, M. Way and W. Witke for critical assessment of the manuscript.

CORRESPONDENCE and requests for materials should be addressed to M.Z. (e-mail: zerial@embl-heidelberg.de). The sequence of RhoD has been deposited in GenBank, accession no. X84325.

Sec61-mediated transfer of a membrane protein from the endoplasmic reticulum to the proteasome for destruction

Emmanuel J. H. J. Wiertz, Domenico Tortorella, Matthew Bogyo, Joyce Yu, Walther Mothes*, Thomas R. Jones†, Tom A. Rapoport* & Hidde L. Ploegh

Center for Cancer Research, Department of Biology, Massachusetts Institute of Technology, Cambridge, Massachusetts 02139, USA
* Department of Cell Biology, Harvard Medical School, Boston, Massachusetts 02115, USA
† Department of Molecular Biology, Infectious Diseases Section, Wyeth–Ayerst Research, Pearl River, New York 10965, USA

The human cytomegalovirus genome encodes proteins that trigger destruction of newly synthesized major histocompatibility complex (MHC) class I molecules. The human cytomegalovirus gene *US2* specifies a product capable of dislocating MHC class I molecules from the endoplasmic reticulum to the cytosol and delivering them to the proteasome. This process involves the Sec61 complex, in what appears to be a reversal of the reaction by which it translocates nascent chains into the endoplasmic reticulum.

CYTOLYTIC T cells eradicate virus-infected cells by recognition of virus-derived peptides in a physical complex with MHC class I molecules[1]. In this way, the cell advertises to the immune system that it harbours a pathogen, and invites its destruction.

The selective pressure exerted by the immune system on viruses has led them to acquire, in the course of their evolution, a set of remarkable strategies with which they can elude cytolytic T cells. Certain viruses inhibit surface expression of class I–peptide complexes, thereby preventing destruction of the host cell in which they replicate[2]. In human cytomegalovirus (HCMV)-infected cells, this mechanism involves the rapid degradation of MHC class I molecules[3,4], a process in which the HCMV genes *US2* and *US11* play a key role[4,5]. Such a multiplicity of mechanisms to cripple MHC class I expression suggests that cytolytic T cells are pivotal in the host defence against HCMV.

MHC class I molecules consist of two subunits, a heavy chain and β_2-microglobulin, whose association is required for peptide binding in the ER and for efficient transport of the complex out of the ER[6]. The heavy chain is targeted to the endoplasmic reticulum (ER) membrane by an amino-terminal, cleaved signal sequence, contains a glycosylated lumenal domain, and has a carboxy-terminal membrane anchor (type I membrane protein). The light chain β_2-microglobulin is a secreted protein with a cleavable signal sequence. Both proteins are translocated across the ER membrane during their synthesis by an apparatus whose major constituent is the Sec61 complex. This membrane protein complex consists of three subunits, α, β, γ, and probably forms a protein-conducting channel[7].

In cells expressing the HCMV *US11* gene product, a type I membrane protein, the heavy-chain molecules are inserted into the ER membrane and are glycosylated cotranslationally, but shortly thereafter they are rapidly transported back into the cytosol, where they are deglycosylated by an *N*-glycanase and degraded by the proteasome[5]. How dislocation of the polypeptide chains occurs is unknown. However, a similar process may also occur in normal cells and may correspond to the process referred to as ER degradation[8,9]. Several membrane proteins that misfold in the ER are degraded following the attachment of ubiquitin[10–13]. Involvement of the ubiquitin pathway[14], and inhibition of breakdown by agents that target the proteasome[15] imply that there is a cytosolic component to such degradation. Again, the mechanism by which these proteins are extracted from the membrane and transferred to the proteasome is unknown.

We have now found a second HCMV gene product, encoded by *US2*, that also triggers dislocation of newly synthesized class I heavy chain molecules into the cytosol for degradation by the proteasome. Characterization of the fate of MHC class I molecules in cells expressing the US2 gene product illuminates the underlying molecular mechanisms. US2 binds to newly synthesized class I molecules and escorts them into the cytosolic compartment where the heavy chains, and possibly US2, are deglycosylated by a *N*-glycanase. The deglycosylated breakdown intermediate is associated with the Sec61 complex, suggesting that retrograde transport occurs through the same protein-conducting channel that allowed the original membrane insertion of the heavy chain. The deglycosylated intermediate is also associated with the